Received: 29 April 2022 | Revised: 8 September 2022 | Accepted: 20 September 2022

DOI: 10.1111/cas.15602

ORIGINAL ARTICLE

Cancer Science WILEY

Metformin and simvastatin synergistically suppress endothelin 1-induced hypoxia and angiogenesis in multiple cancer types

Jie Liu[1,2] | Huxia Wang[1,3] | Miao Zhang[1,2] | Yazhao Li[1,2] | Ruiqi Wang[1,2] | He Chen[1,2] | Bo Wang[1,2] | Xiaoqian Gao[1,2] | Shaoran Song[1,2] | Yaochun Wang[1,2] | Yu Ren[4] | Juan Li[1,2] | Peijun Liu[1,2]

[1]Center for Translational Medicine, The First Affiliated Hospital of Xi'an Jiaotong University, Xi'an, Shaanxi Province, China

[2]Key Laboratory for Tumor Precision Medicine of Shaanxi Province, The First Affiliated Hospital of Xi'an Jiaotong University, Xi'an, Shaanxi Province, China

[3]Mammary Department, Shaanxi Provincial Cancer Hospital, Xi'an, Shaanxi Province, China

[4]Department of Surgical Oncology, The First Affiliated Hospital of Xi' an Jiaotong University, Xi'an, Shaanxi Province, China

Correspondence
Peijun Liu and Juan Li, First Affiliated Hospital of Xi'an Jiaotong University, Xi'an, 710061, Shaanxi Province, China.
Emails: liupeijun@xjtu.edu.cn; lijuanxjtu@xjtu.edu.cn

Yu Ren, Department of Surgical Oncology, First Affiliated Hospital of Xi'an Jiaotong University, Xi'an, 710061, Shaanxi Province, China.
Email: renyyyyy@126.com

Funding information
Clinical Research Award of the First Affiliated Hospital of Xi'an Jiaotong University, Grant/Award Number: XJTU1AF-CRF-2017-007; Key Research and Development Projects of Shaanxi Province, Grant/Award Number: 2020SF-038 and 2021SF-121; National Natural Science Foundation of China, Grant/Award Number: 81703002 and 81872272; The MET

Abstract

Multiple cancers have been reported to be associated with angiogenesis and are sensitive to anti-angiogenic therapies. Vascular normalization, by restoring proper tumor perfusion and oxygenation, could limit tumor cell invasiveness and improve the effectiveness of anticancer treatments. However, the underlying anticancer mechanisms of antiangiogenic drugs are still unknown. Metformin (MET) and simvastatin (SVA), two metabolic-related drugs, have been shown to play important roles in modulating the hypoxic tumor microenvironment and angiogenesis. Whether the combination of MET and SVA could exert a more effective antitumor effect than individual treatments has not been examined. The antitumor effect of the synergism of SVA and MET was detected in mouse models, breast cancer patient-derived organoids, and multiple tumor cell lines compared with untreated, SVA, or MET alone. RNA sequencing revealed that the combination of MET and SVA (but not MET or SVA alone) inhibited the expression of endothelin 1 (ET-1), an important regulator of angiogenesis and the hypoxia-related pathway. We demonstrate that the MET and SVA combination showed synergistic effects on inhibiting tumor cell proliferation, promoting apoptosis, alleviating hypoxia, decreasing angiogenesis, and increasing vessel normalization compared with the use of a single agent alone. The MET and SVA combination suppressed ET-1-induced hypoxia-inducible factor 1α expression by increasing prolyl hydroxylase 2 (PHD2) expression. Furthermore, the MET and SVA combination showed a more potent anticancer effect compared with bosentan. Together, our findings suggest the potential application of the MET and SVA combination in antitumor therapy.

KEYWORDS
angiogenesis, ET-1, hypoxia, metformin, simvastatin

Jie Liu and Huxia Wanghese contributed equally to this study.

1 | INTRODUCTION

Angiogenesis is a complex process involving multiple genes expressed by different cells.[1,2] Hypoxia plays a major role in angiogenesis and regulates genes in multiple stages of angiogenesis.[3] As a result of unlimited tumor growth, the hypoxic microenvironment reprograms the metabolic phenotypes of tumor cells to maintain their survival and proliferation. Hypoxia-inducible factor (HIF) is the key transcriptional regulator of tumor angiogenesis and hypoxic stress. High expression of hypoxia-inducible factor 1α (HIF1α) has been detected in many human cancers and is closely correlated with tumor initiation, growth, metabolism, angiogenesis, invasion, inflammatory cell recruitment and metastasis, and poor patient prognosis.[3–5] Promoted blood vessel normalization through improved pericyte coverage and restoration of cell junctions leading to increased tumor perfusion would limit tumor hypoxia and prevent the selection of tumor cells with a more invasive phenotype; these events would improve the distribution and efficiency of anticancer treatments.[6] A variety of tumor therapies and inhibitors have been designed to target HIF and angiogenesis-related pathways, and many of these treatments have entered clinical trials and clinical application.[7,8]

Metformin (MET) is the first-line medication for type 2 diabetes. Several studies have shown that MET also inhibits the growth of many types of tumors, such as breast cancer and hepatocellular carcinoma. MET was shown to exhibit antitumor activities such as cell growth inhibition and induction of apoptosis by inhibiting the Warburg effect and alleviating hypoxia.[9–12] Statins such as simvastatin (SVA) are the first-line treatment for decreasing cholesterol levels and cardiovascular disease. Many reports, including our previous studies, showed that statins also exhibit antitumor effects. For example, statins have been demonstrated to prevent colorectal cancer, inhibit the proliferation of breast cancer cells, induce apoptosis, and block the invasion and metastasis of human melanoma cells.[13–17] However, whether the combination of SVA and MET exerts more effective antitumor activities compared with single-agent treatments has not been explored.

In this study, we investigated the antitumor potential of the combination treatment of MET and SVA against multiple tumor types. We found that the MET and SVA combination exerted a synergistic effect to significantly inhibit the growth of various types of tumors and breast cancer patient-derived organoids (PDOs). The MET and SVA combination induced the apoptosis of tumor cells, alleviated hypoxia, inhibited angiogenesis, and increased vessel normalization to a greater extent than either MET or SVA alone. Our findings indicate that the MET and SVA combination treatment represents a potential therapeutic strategy for antitumor treatment.

2 | MATERIAL AND METHODS

2.1 | Cell lines and cell culture

Human hepatocarcinoma cell lines HepG2 and Hep3B, breast cancer cell lines MCF-7 and MDA-MB-231, human lung cancer cell line H1299, cervical cancer cell lines SiHa and C33A, and murine mammary carcinoma cell 4T1 were cultured in high glucose Dulbecco's Modified Eagle's medium (HyClone) supplemented with 10% fetal bovine serum (HyClone). Human lung cancer cell line A549 and murine melanoma cell line B16 and Roswell Park Memorial Institute (RPMI)-1640 medium (HyClone) supplemented with 10% fetal bovine serum. All cells were maintained at 37°C and 5% CO_2 in an incubator. The cell lines were obtained from the China Infrastructure of Cell Line Resource (Beijing, China). MET and endothelin 1 (ET-1) were obtained from Aladdin. SVA and Bosentan were obtained from Selleck. In experiments conducted under anoxia conditions, cells were cultured in a 1% O_2, 5% CO_2 incubator for 24 h.

2.2 | Colony formation assays

Cells were treated with MET and/or SVA for 24 h and then reseeded into new plates. The cells were then cultured for 14 days, followed by fixing using 4% paraformaldehyde (PFA) and staining with 0.5% crystal violet, as described previously.[11]

2.3 | Apoptosis assays

Treated cells were collected and analyzed using the Annexin V-PE apoptosis detection kit (BD Biosciences) and flow cytometry (BD Biosciences). Assays were performed following the manufacturer's instructions.

2.4 | Western blotting

Treated cells were lysed in radio immunoprecipitation assay buffer, and the lysates were separated by sodium dodecylsulphate polyacrylamide gel electrophoresis and transferred onto a polyvinylidene fluoride membrane. The membrane was blocked with 5% fat-free milk in tris-buffered saline and tween 20 and then incubated with primary antibody, followed by incubation with horseradish peroxidase -conjugated secondary antibody (1:10000; Proteintech). The chemiluminescent signals were detected using ChemiDoc™ XRS+ (Bio-rad). The primary antibodies anti-phospho-retinoblastoma (1:1000), anti-retinoblastoma (1:1000), anti-cleaved caspase3 (1:1000), anti-caspase3 (1:1000), and anti-Hypoxia inducible factor 1 subunit alpha (1:1000) were obtained from Cell Signaling Technology. Anti-Minichromosome maintenance complex component 7 (1:1000), anti-endothelin 1 (1:1000), and anti-prolyl hydroxylase 2 (PHD2) (1:1000) were purchased from Santa Cruz, anti-endothelin receptor A (ETAR) (1:1000) was purchased from Abcam, and anti-endothelin receptor B (ETBR) (1:1000), anti-survivin (1:1000), and β-actin (1:10000) were purchased from Proteintech.

2.5 | Mouse models

Female BALB/cAnNCrl mice (4–6 weeks old, $n = 6$) and C57BL/6J mice (4–6 weeks old, $n = 6$) were obtained from Xi'an Jiaotong

University. All animal procedures were performed according to the protocol approved by the Institutional Animal Care and Use Committee at Xi'an Jiaotong University.

In experiments with BALB/cAnNCrl mice, 5×10^5 4T1 cells were injected into the fat pad of the fourth left mammary gland of mice. In experiments with C57BL/6J mice, 1×10^6 B16 cells were subcutaneously injected into mice. Mice were randomized into four groups: control, SVA, MET, or MET and SVA in combination ($n = 6$ for each group). The mice were then treated with 15 mg/kg/day SVA and/or 100 mg/kg/day MET by intragastric administration. Mice were monitored every 2 days for 2 weeks. At the end of the experiment, mice were sacrificed and tumors were harvested for subsequent analysis.

2.6 | Immunohistochemistry

Immunohistochemistry and quantification were performed as described previously.[11,12] Briefly, tissues were fixed in 10% neutralized formaldehyde and embedded in paraffin. Tissues were then sectioned and stained with primary antibodies against proliferating cell nuclear antigen (PCNA) (1:500; Santa Cruz) and cleaved caspase-3 or HIF1α (1:200; Cell Signaling Technology). Images were taken using a Leica SCN400 slide scanner.

2.7 | Immunofluorescence

Immunofluorescence was performed as described previously.[11] Briefly, cells or mouse tissues were fixed by 4% PFA and permeabilized with 0.5% Triton X-100 in phosphate belanced solution, followed blocking with 5% bovine serum albumin supplemented with 10% goat serum. Samples were stained with primary antibodies against platelet and endothelial cell adhesion molecule 1 (1:50; Abcam), neural/glial antigen-2 (1:100; BD Biosciences), vascular epithelium (1:100; Biolegend), HIF1α (1:100; Cell Signaling Technology), and ETBR (1:100; Abcam). Nuclei were stained with 4, 6-diamidino-2-phenylindone (DAPI; 5 μg/ml). Images were taken by confocal laser scanning microscopy (Leica TCS SP5).

Lectin (20 mg/kg) was intravenously injected into mice and then the mice received intracardiac perfusion of 40 ml of 4% PFA with a flux of 10 ml/min. Tumors were extracted and fixed with 4% PFA, embedded at optimal cutting temperature (OCT) (Sakura Finetek), and sectioned. The samples were co-stained with CD31 and rhodamine-labeled lectin (Vector Labs) for 15 min. Images were acquired by confocal laser scanning microscopy.

Next, 60 mg/kg body weight pimonidazole HCl (PIMO; Hypoxyprobe Inc.) was intravenously injected into the tail vein of tumor-bearing mice 90 min before tumors were extracted. Then, the $PIMO^+$ hypoxic cells were immunostained with anti-PIMO antibody (Hypoxyprobe Inc.) following the manufacturer's instructions.

2.8 | RNA sequencing

HepG2 cells were treated with 2.5 μM SVA, 5 mM MET, or a combination of 2.5 μM SVA and 5 mM MET for 24 h. Untreated cells were used as controls. The cells were then harvested and cryopreserved in liquid nitrogen. RNA sequencing (RNA-seq) was performed Guangzhou RiboBio. The data were analyzed by Gene Denovo. Each group contained three independent samples for gene expression analysis.

2.9 | PDO model

Breast cancer tissues from eight patients were obtained from the First Affiliated Hospital of Xi'an Jiaotong University with informed consent from the patients. The experimental procedures were approved by the Ethics Review Committee of the First Affiliated Hospital of Xi'an Jiaotong University. PDOs were established as described previously.[18] Briefly, the breast cancer tissues were chopped up and digested by collagenase at 37 °C for 1 h and then filtered through a 150 mesh filter and centrifuged for 10 min at 400 × *g*. The precipitate was resuspended in organoid medium and then centrifuged again. The pellet was resuspended with 40 μl BME type 2 hydrogel (Trevigen). After the BME solidified, 400 μl of organoid medium was added into each well for PDO culture.

2.10 | Statistical analysis

Quantitative analyses were performed using Prism 7.0 software. Data are shown as mean ± SEM. Statistical significance was calculated using two-tailed Student's *t*-test or two-way ANOVA *t*-test. Each set of experimental data represents a minimum of three biological replicates. A *P* value less than 0.05 was considered statistically significant.

3 | RESULTS

3.1 | Combination of MET and SVA alleviates hypoxia and inhibits angiogenesis

Hypoxia facilitates metabolic reprogramming in tumors, which is feature of tumors.[3,19] The metabolic reprogramming in cancer allows tumors to use glucose and lipids as energy sources.[20] MET[9–12] and SVA[13–15,17] are clinically used to reduce glucose and lipids,[17,21–23] and studies have shown that they inhibit growth and induce the apoptosis of tumor cells in vitro and in vivo.[24] We examined whether the combination of MET and SVA could exert a more effective antitumor effect than individual treatments. We therefore explored the effects of the combination treatment in vivo by injecting 4T1 or B16 cells into mice and treating the mice with the single or combination

agents. We first examined the hypoxic areas of 4T1 and B16 tumors from the treatment groups by costaining for PIMO (Hypoxyprobe, a reagent for detecting hypoxia) and HIF1α. In 4T1 tumors, the tumors from the combination treatment group showed a 50% reduction in the hypoxic area compared with the control group, and a 25%–35% reduction in hypoxic area compared with the single treatment groups. In B16 tumors, we observed a decrease in the hypoxic area of more than 60% compared with the controls and a 40%–50% reduction compared with the single treatments (Figure 1A,B). In line with the in vivo results, the combination treatment inhibited HIF1α expression in cells cultured under hypoxic conditions (1% O_2) and 4T1 and B16 tumors (Figures 1C and S1). In 1992, vascular endothelial growth factor (VEGF) probably plays as a hypoxia-inducible angiogenic factor,[25] thus we also found the combination treatment inhibited HIF1α-induced VEGF expression (Figure 1C). Together these findings indicate that the combination treatment led to reduced hypoxia in tumors.

To more closely investigate the mechanism underlying the antitumor effect of the MET and SVA combination, we performed RNA-seq in HepG2 cells treated with SVA or MET alone or in combination. Compared with the vehicle group, we identified genes that only showed greater than 2-fold changes in cells treated with the MET and SVA combination but did not show differences in response to MET or SVA alone. Gene Ontology analysis was performed to determine the top 8 biological processes enrichment terms in genes from the MET and SVA combination group. The results showed enrichment in terms related to angiogenesis, blood vessel development and morphogenesis, and vasculature development (Figure 1D). These findings suggest that the antitumor activities of the MET and SVA combination may involve effects on angiogenesis.

Excessive angiogenesis and immature vasculature are characteristic features of tumors and are closely related to the hypoxic tumor microenvironment. Angiogenesis plays a critical role in cancer progression, and anti-angiogenic therapies are currently widely used as antitumor therapies.[26–28] We examined the expression of platelet endothelial cell adhesion molecule (PECAM-1 or CD31), a marker of vessel endothelial cells,[29] in tumor sections from the mouse treatment groups established above. We observed a dramatic decrease in both the numbers of vessels and branch points in tumors as detected by CD31 staining in the combination group compared with the single-treatment and control groups (Figure 1E–J). Together, these results suggest that the MET and SVA combination may play a role in inhibiting tumor angiogenesis.

3.2 | Combination of MET and SVA promotes vessel normalization

VEGF is a major driver of angiogenesis and has become a critical target for antitumor treatment strategies. However, in preclinical studies, anti-VEGF therapy induces tumor vasculature, showing a more "mature" or "normal" phenotype with attenuated hyperpermeability, increased vascular pericyte coverage, and a normal basement membrane. Endothelial cells lining tumor vessels show regular and organized morphology and stain for CD31. Vascular normalization might enhance the benefits of host antitumor immune responses and conventional cancer treatments.[29] We found a similar phenomenon in our immunofluorescence results: while fewer vessels were detected in the combination group, the length of the CD31-stained vessels appeared to be longer than that in other treatment groups (Figure 1B,E).

NG2 is a marker of pericytes and vascular endothelial (VE)-cadherin is an endothelial-specific adhesion molecule.[29] We found that both NG2 and VE-cadherin showed increased expression in $CD31^+$ vessels after the MET and SVA combination group compared with the single-treatment groups (Figure 2A–D).

Lectin binds the surface of endothelial cells along the blood flow. We found that lectin-positive vessels were also increased in the MET and SVA combination group compared with the controls (Figure 2E,F). Together these results suggest that the MET and SVA combination inhibited disorganized and nonfunctional vessels, and promoted vessel normalization and maturity.

3.3 | Combination treatment of MET and SVA inhibits tumor growth in vivo

We found that the combination treatment showed potent antiproliferation effects in cancer cells in vitro. The mouse model groups treated with SVA, MET or the combination showed a reduction in tumor growth and improved survival compared with the controls (Figure 3A–F). Notably, the inhibition of tumor growth and prolonged survival of mice was enhanced in the group treated with the combination of MET and SVA compared with the groups treated with MET or SVA alone. Immunohistochemical analysis of tumors from each group showed increased cleaved caspase 3 expression and decreased PCNA expression in the combination treatment group compared with levels in the other groups (Figures 3G,H and S1).

FIGURE 1 The effects of MET and SVA on hypoxia and angiogenesis. Costaining of HIF1α and PIMO (A) and quantification of hypoxic area (B) of 4T1 tumors and B16 tumors. Bar = 50 μm. (C) Western blotting of HIF1α and VEGF in HepG2, Hep3B, MCF7, and MDA-MB-231 cells cultured under hypoxic conditions and treated as indicated. (D) The transcriptomes of HepG2 cells treated with vehicle, SVA, MET or the combination of SVA and MET were determined by RNA sequencing. We identified genes that only showed changes after treatment with the SVA and MET combination but did not show differences in response to SVA or MET by a trend analysis. The top 10 biological process enrichment terms in the SVA and MET combination group by Gene Ontology (GO) analysis were determined. Immunofluorescence was performed for CD31, a vessel marker, in 4T1 tumors (E) and B16 tumors (H) from the treatment groups described above. Bars = 100 μm. The vessel numbers and branch points in 4T1 tumors (F, G) and B16 tumors (I, J) from the indicated groups were determined. $^{**}P < 0.01$, $^{***}P < 0.001$.

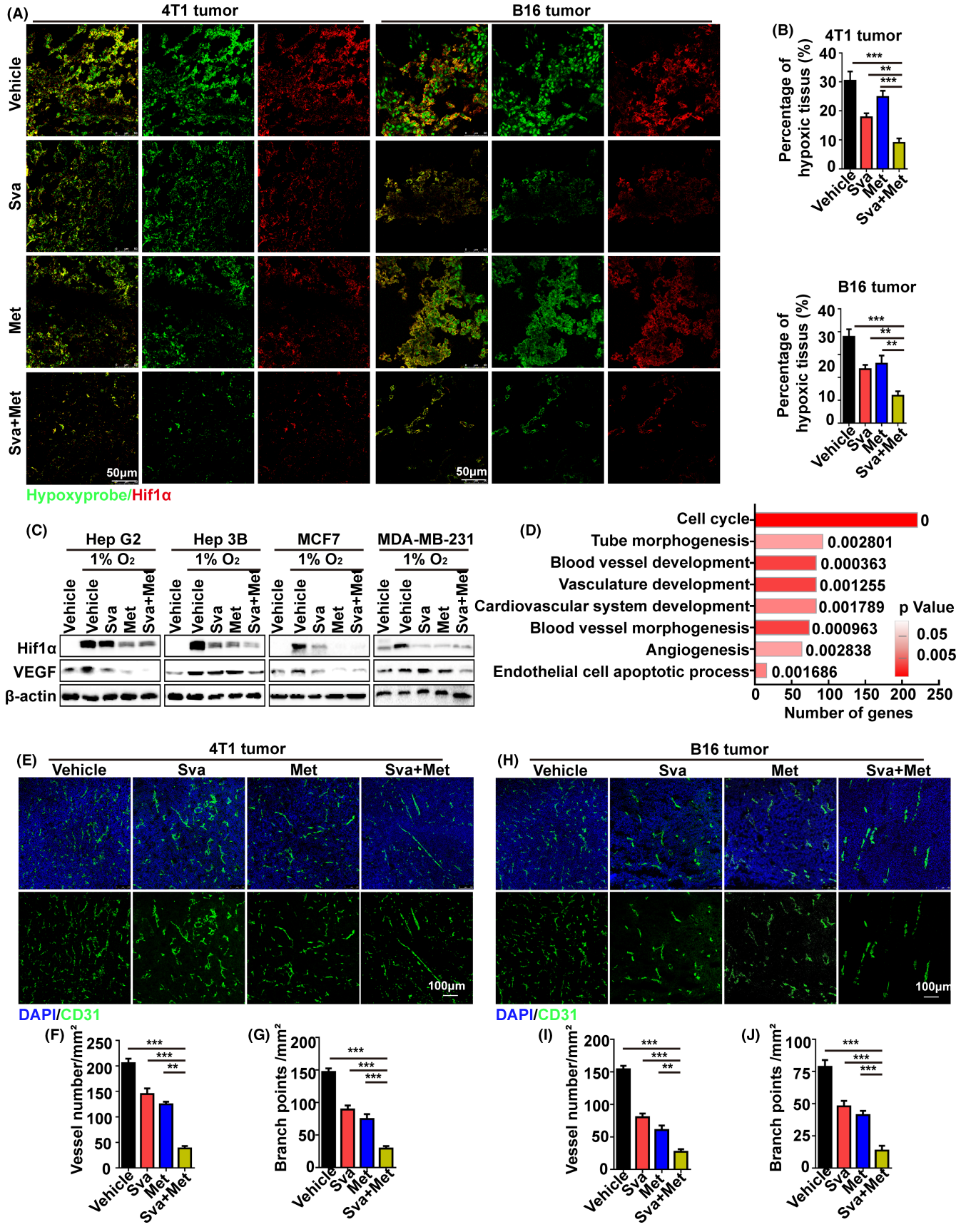
(A)
4T1 tumor
B16 tumor
Vehicle
Sva
Met
Sva+Met
50μm
Hypoxyprobe/Hif1α
(B)
4T1 tumor
Percentage of hypoxic tissus (%)
B16 tumor
(C)
Hep G2
Hep 3B
MCF7
MDA-MB-231
1% O2
Hif1α
VEGF
β-actin
(D)
Cell cycle
Tube morphogenesis
Blood vessel development
Vasculature development
Cardiovascular system development
Blood vessel morphogenesis
Angiogenesis
Endothelial cell apoptotic process
p Value
Number of genes
(E)
4T1 tumor
100μm
DAPI/CD31
(F)
Vessel number/mm2
(G)
Branch points /mm2
(H)
B16 tumor
(I)
(J)

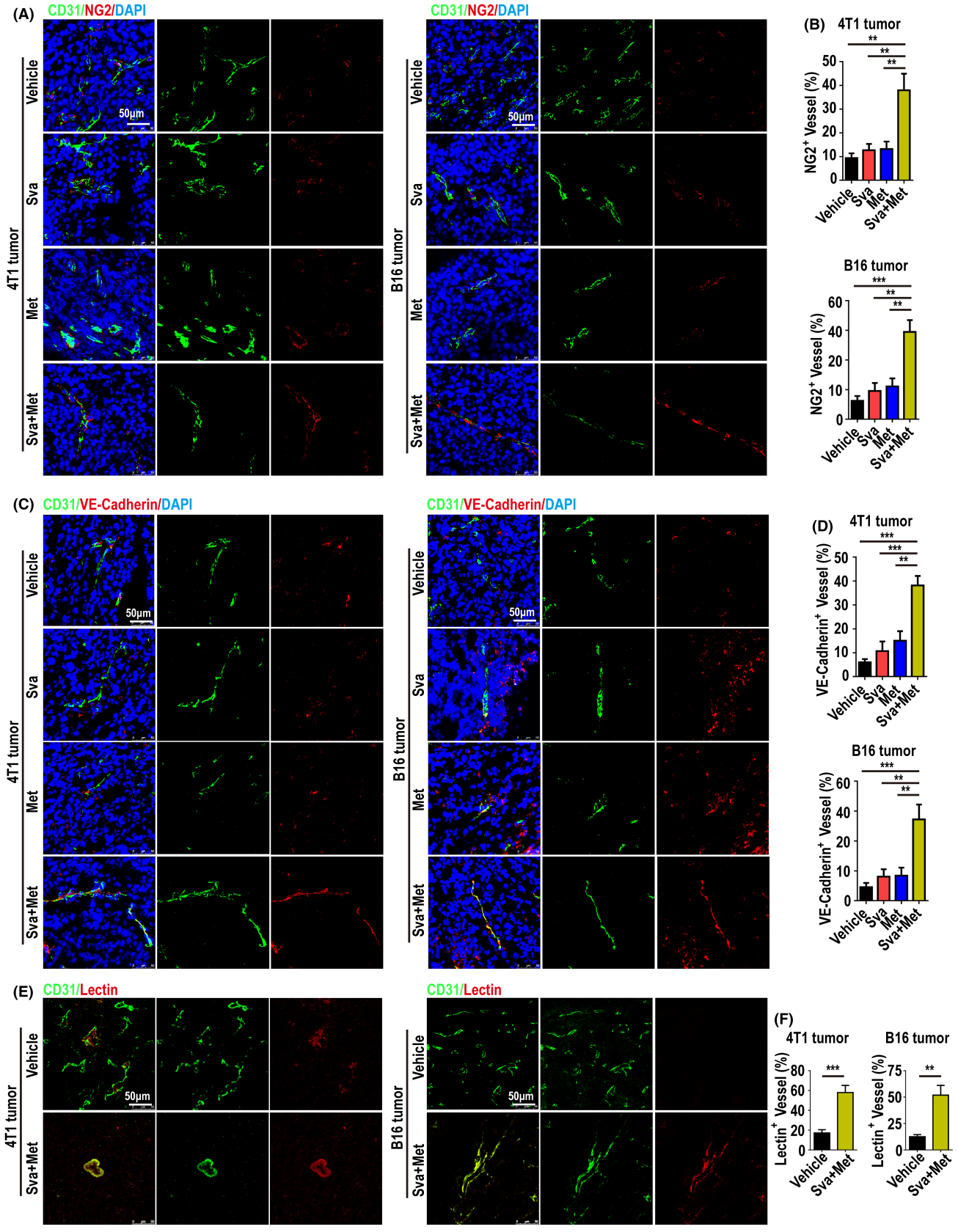

FIGURE 2 Vessel maturity and functional status in response to MET and SVA combination treatment. Immunofluorescence and of CD31 (green) and NG2 (red) of frozen sections of 4T1 tumors and B16 tumors from the indicated groups (A) and their quantification (B). Immunofluorescence of CD31 (green) and VE-cadherin (red) of frozen sections of 4T1 tumors and B16 tumors from the indicated groups (C) and their quantification (D). Lectin-perfused $CD31^+$ vessels in frozen sections of 4T1 tumors and B16 tumors in the indicated groups (E) and their quantification (F). Bar = 50 μm.

Together, these results indicated that the combination treatment showed potent effects in inhibiting tumor growth and inducing the apoptosis of tumor cells in vivo.

3.4 | Combination treatment of MET and SVA shows a synergistic anticancer effect in vitro

Next, we examined the effects of MET and SVA alone or in combination on the proliferation of various types of tumor cell lines in vitro using liver cancer cell lines (HepG2, Hep3B), lung cancer cell lines (A549, H1299), and cervical cancer cell lines (SiHa, C33A) (Figures 4A and S2, Table 1). Both MET and SVA individually showed growth inhibitory effects on the cell lines to varying degrees. Notably, the combination treatment showed potent growth inhibitory effects compared with the individual treatments, with a moderate to strong synergistic effect.[30] We previously showed that SVA inhibits phosphorylated retinoblastoma (RB) and mini-chromosome maintenance protein 7 (MCM7) expression to suppress tumor cell growth.[14] The MET and SVA combination treatment resulted in a dramatic decrease in p-RB and MCM7 levels (Figure 4B). Similarly to our previously research on SVA treatment in the regulation of cell cycles, the MET and SVA combination treatment also can reduced the percentages of the G2/M phase cells (Figure S3).

We next evaluated the effect of the individual and combination treatments on the apoptosis of HepG2, Hep3B, MCF7, and MDA-MB-231 cancer cell lines. Similar to the cell proliferation results, while the individual treatments induced apoptosis, the combination treatment resulted in markedly increased apoptosis in all cell lines compared with the individual treatments with synergistic effects (Figure 4C,D). Survivin is a novel anti-apoptosis gene, and knockdown of survivin expression induces cell apoptosis through activation of caspase-3.[31–33] The induction of apoptosis was accompanied by the elevation of cleaved caspase 3 and downregulated survivin levels (Figure 4E). Together, these results demonstrate that the MET and SVA combination exhibits potent effects on suppressing cancer cell proliferation and inducing apoptosis to levels higher than the individual treatments alone.

3.5 | MET and SVA synergistically inhibit the ET-1-HIF1α signaling axis

KEGG pathway analysis of RNA-seq in HepG2 cells identified the relaxin and HIF1α signaling pathways in the data from the MET and SVA combination group. The HIF1α transcription factor is a critical regulator of hypoxia and plays key roles in various aspects of tumor development, including angiogenesis. *EDN1*, which encodes endothelin 1 (ET-1),[34] an important regulator of the HIF1α signaling pathway, was markedly decreased in cells treated with the combination treatment compared with controls (Figure 5A). We further found that ET-1 and its receptor ETBR were reduced by the combination treatment in vivo and in vitro, but no changes were observed in the expression of ETAR (Figure 5B–D).

Our data showed that the combination treatment led to a decrease of ET-1 expression and HIF1α levels. Under normoxic conditions, PHD2 catalyzes the hydroxylation of HIF1α, leading to its proteasomal degradation.[4] Furthermore, ET-1 stabilizes HIF1α by inhibiting PHD2.[35,36] Treatment of HepG2 and MCF7 cells with ET-1 resulted in inhibited PHD2 expression and induced HIF1α levels, along with upregulated expression of ETBR (Figure 6A). The combination treatment prevented the effects of ET-1 on inducing ETBR and HIFα expression, and increased PDH2 expression (Figure 6B). HIF1a can increase transcriptional expression of the survivin gene.[37,38] Hence, we also found that MET and SVA combination treatment inhibited ET1-induced survivin expression (Figure 6A,B). Immunofluorescence showed that ET-1-induced HIF1α protein was localized in the nucleus and reduced by the combination treatment (Figures 6C and S3). HIF1α is a key transcriptional regulator of molecules in angiogenic pathways. The decrease in HIF1α expression is associated with inhibition of tumor angiogenesis.

Bosentan is an endothelin receptor antagonist that targets ETAR and ETBR, and has been evaluated in clinical oncology for metastatic melanoma.[39–41] The combination treatment suppressed ET-1-induced HIF1α, ETBR and survivin expressions at a level similar to the inhibition of ETBR by bosentan or knockdown by small interfering RNAs (Figures 6D and S4). The combination of SVA and MET also displayed a stronger inhibition on cell proliferation compared with bosentan (Figure 6E). This suggests that the MET and SVA combination inhibits ET-1-induced hypoxia.

3.6 | The MET and SVA combination suppresses growth and ET-1-induced HIF1α expression of breast cancer PDOs

PDO models have expanded the cell-line- and xenograft-based research of cancer and drug development. These models have been used to directly and rapidly test drug sensitivity and facilitate the identification of personalized tumor therapy.[18,42] To explore the potential application of the combination of MET and SVA in cancer treatment, we first established breast cancer PDOs from eight patients and confirmed that the PDOs readily expanded. Hematoxylin and eosin staining was performed on paraffin sections of patient tumors, and the results confirmed that the histopathological features of breast cancer PDOs showed a strong concordance with that of the corresponding parental tumor (Figure 7A and Table S1). The MET and SVA combination treatment dramatically inhibited the viability and volume of breast cancer PDOs compared with that of the single treatments (Figure 7B–D). The expressions of ET-1 and ETBR were also suppressed by the combination treatment (Figure 7E,F). Furthermore, ET-1-induced HIF1α expression was inhibited by the combination treatment to a similar extent to that of bosentan (Figure 7G).

A schematic for our proposed model is shown in Figure 7H. We propose that the MET and SVA combination treatment induces its antitumor effects by inhibiting ET-1-induced HIF1α expression and blocking the effects of HIF1α on promoting angiogenesis and suppressing apoptosis.

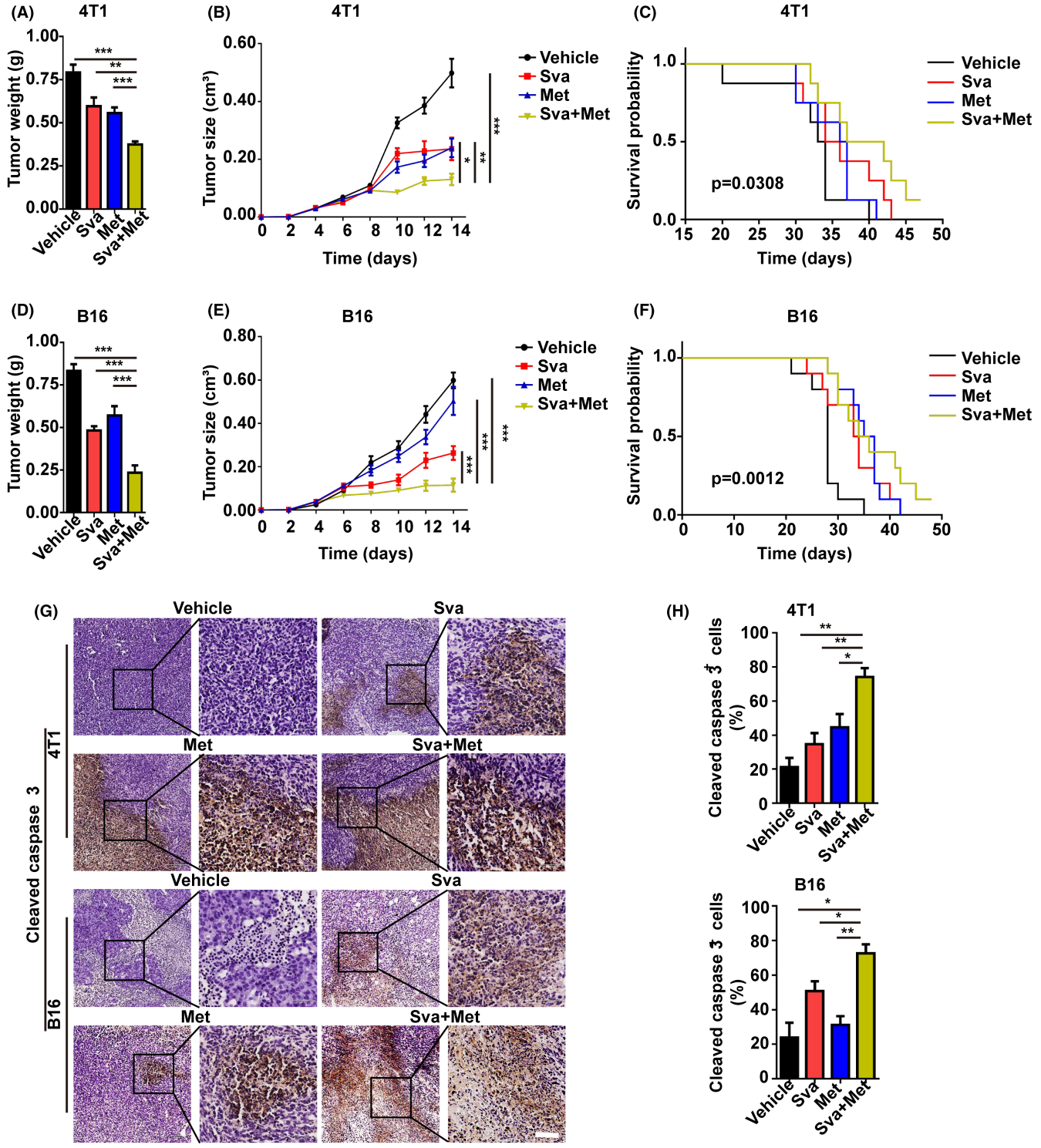

FIGURE 3 Inhibitory effects of the combination treatment of MET and SVA on tumor growth and mouse survival in vivo. BALB/cAnNCrl mice were injected with 4T1 cells and treated with 15 mg/kg/day SVA, 100 mg/kg/day MET, or the combination of 15 mg/kg/day SVA and 100 mg/kg/day MET ($n = 6$ per group). C57BL/6J mice were injected with B16 cells and treated with 15 mg/kg/day SVA, 100 mg/kg/day MET or the combination of 15 mg/kg/day SVA and 100 mg/kg/day MET ($n = 6$ per group). Tumor weight (A, D), tumor growth (B, E), and survival (C, F) of the individual groups were recorded. (G, H) Immunohistochemistry staining of cleaved caspase 3 in 4T1 and B16 tumors. Bar = 50 μm. $^{*}P < 0.05$, $^{**}P < 0.01$, $^{***}P < 0.001$.

4 | DISCUSSION

In this study, we demonstrated that the MET and SVA combination showed synergistic antitumor effects compared with either MET or SVA alone. The MET and SVA combination treatment was found to inhibit the growth of tumor cells, promote the apoptosis of tumor cells, inhibit angiogenesis, promote vessel normalization, and alleviate hypoxia. Our results indicate that the MET and SVA combination

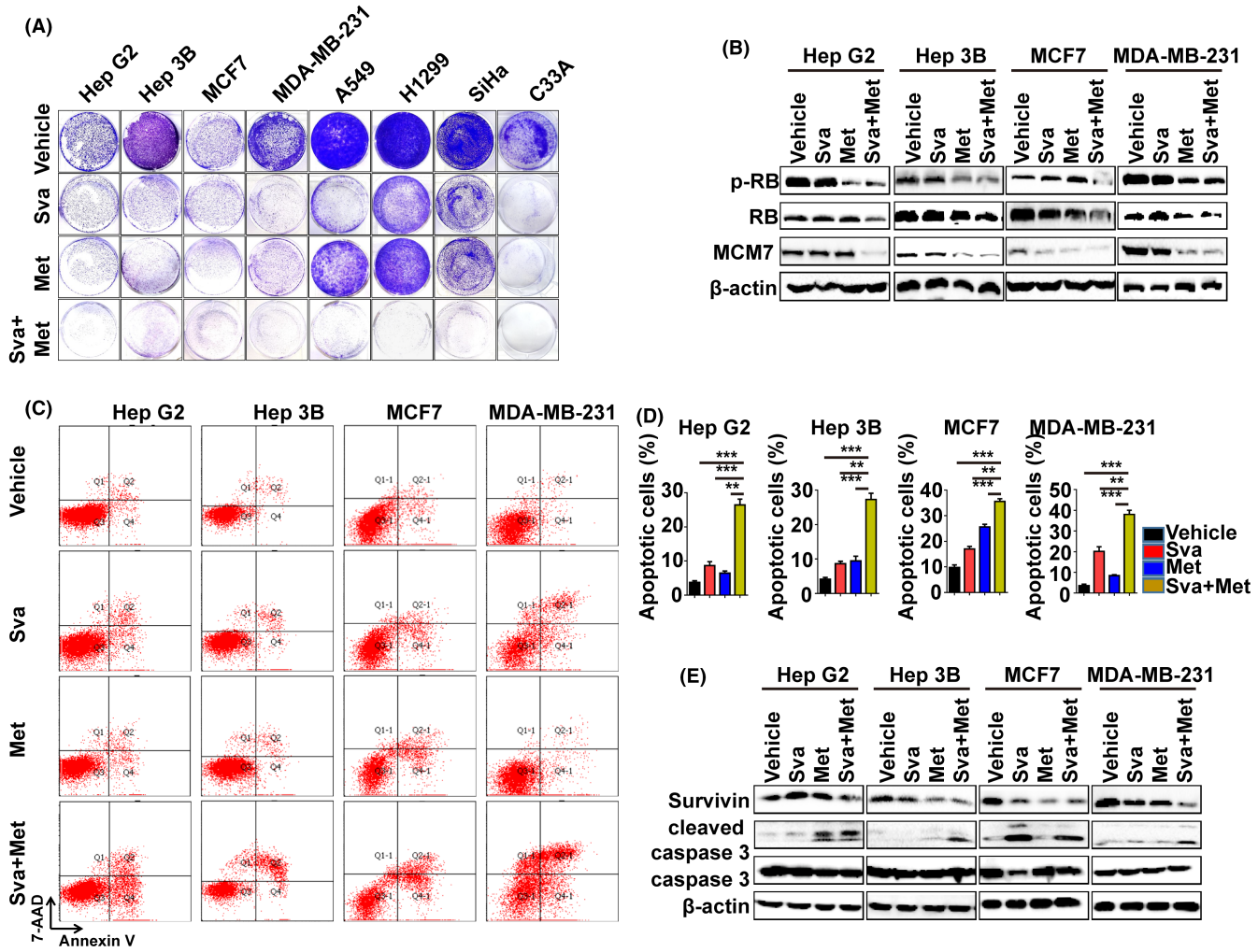

FIGURE 4 Inhibitory effects of the combination treatment of MET and SVA on cancer cells. (A) Colony formation assays were performed in HepG2, Hep3B, A549, H1299, SiHa, and C33A cells treated with 2.5 μM SVA, 5 mM MET or the combination of 2.5 μM SVA and 5 mM MET for 24 h as well as MCF7 and MDA-MB-231 cells treated with 1 μM SVA, 10 mM MET or the combination of 1 μM SVA and 10 mM MET for 24 h. Images were obtained after 14 days of culture. (B) Western blotting of the indicated proteins in HepG2, Hep3B, MCF7, and MDA-MB-231 cells treated with SVA, MET or the combination of SVA and MET. (C, D) The percentages of apoptotic cells in HepG2 and Hep3B cells treated with 2.5 μM SVA, 5 mM MET or the combination of 2.5 μM SVA and 5 mM MET for 24 h as well as MCF7 and MDA-MB-231 cells treated with 1 μM SVA, 10 mM MET or the combination of 1 μM SVA and 10 mM MET for 24 h. (E) Western blot analysis of the indicated proteins in HepG2, Hep3B, MCF7, and MDA-MB-231 cells treated with SVA, MET or the combination of SVA and MET. $^{**}P < 0.01$, $^{***}P < 0.001$.

may exert its effects through the prominent inhibition of ET-1/ETBR expression, and subsequently suppression of expression and nuclear localization of ET-1-induced HIF1α.

A previous study examined the combination treatment of MET and SVA in polycystic ovary syndrome.[43] Other studies explored the combination treatment and the related cancer inhibitory activity in prostate cancer, colorectal cancer, hepatocellular carcinoma, and endometrial cancer.[44–51] Our results demonstrated that the MET and SVA combination treatment showed a wide range of anticancer effects in breast cancer, hepatocellular carcinoma, lung cancer, and cervical cancer. In addition, we confirmed that SVA combined with MET resulted in synergistic antitumor effects compared with the use of SVA or MET alone.

The combination treatment of MET and SVA induced apoptosis and inhibited proliferation,[44,45] which was regulated by increasing the catalytic activity of AMPKα and expression of the phosphatase and tensin homolog (PTEN) tumor suppressor.[50,51] In our study, we found that the MET and SVA combination inhibited cell growth, accompanied by decreased RB and MCM7 expression, and promoted apoptosis, accompanied by increased cleaved-caspase 3 and decreased survivin.

Angiogenesis is a critical hallmark of cancer.[27] We previously showed that MET or SVA as single agents inhibited tumor angiogenesis and induced vessel normalization.[12,16,52] In this study, we found that the MET and SVA combination treatment inhibited angiogenesis and promoted the integrity of the vascular structure and functional

normalization in a synergistic manner, with greater effects than MET or SVA alone, in tumors of orthotopically transplanted mice. RNA-seq results revealed that the gene encoding ET-1 was downregulated in cells treated with the MET and SVA combination treatment. ET-1 plays an important role in mitosis of blood vessel endothelial cells, fibroblasts, vascular smooth muscle cells, and pericytes, and it is highly expressed in many tumors. The ETBR receptor for ET-1 also regulates the proliferation of blood vessel endothelial cells.[34] ET-1 promotes tubular network formation through ETBR in melanoma cells.[34,53,54] Here, we found that the MET and SVA combination treatment led to reduced ET-1 and ETBR expression levels in vitro and in vivo. Thus, inhibition of ET-1-ETBR-mediated angiogenesis may represent a new important antitumor strategy.

In tumors, hypoxic conditions can lead to the induction of angiogenesis, resistance of apoptosis, and promotion of cell proliferation, a process that is regulated by HIF1α.[3] Our findings demonstrated that the MET and SVA combination treatment led to decreased hypoxia area, inhibited growth, and induced apoptosis in tumors. ET-1 stabilizes HIF1α by inhibiting PHD2 expression to control the tumor hypoxic environment.[35,36] Our results shown that ET-1 induced ETBR and HIF1α expression, accompanied by a downregulation of PHD2 and subsequently an upregulation of survivin. MET and SVA combination treatment downregulated ET1-induced HIF1α expression in vivo and in vitro. Consequently, we speculated that MET and SVA combination treatment inhibited angiogenesis and cell proliferation, and induced apoptosis. However, hypoxia also upregulates ET-1 expression.[55] One study showed that survivin attenuated hypoxia-induced transcriptional induction of ET-1 by increasing the polyubiquitination of HIF1α, reducing HIF1α levels and thereby decreasing the amount of HIF1α available to bind to the ET-1 gene promoter.[56] Whether or not the MET and SVA combination treatment

TABLE 1 Effects of simvastatin and metformin on cancer cell lines

Cell line	Combination index (CI_{50})[a]	
HepG2	0.458	Synergism
Hep3B	0.325	Strong synergism
MCF7	0.5	Synergism
MDA-MB-231	0.625	Moderate synergism
A549	0.35	Strong synergism
H1299	0.375	Strong synergism
SiHa	0.72	Moderate synergism
C33A	0.75	Moderate synergism

[a]$CI_{50} > 1.3$ (antagonism); $1.3 \geq CI_{50} > 1.1$ (moderate antagonism); $1.1 \geq CI_{50} > 0.9$ (additive effect); $0.9 \geq CI_{50} > 0.8$ (slight synergism); $0.8 \geq CI_{50} > 0.6$ (moderate synergism); $0.6 \geq CI_{50} > 0.4$ (synergism); $0.4 \geq CI_{50} > 0.2$ (strong synergism).

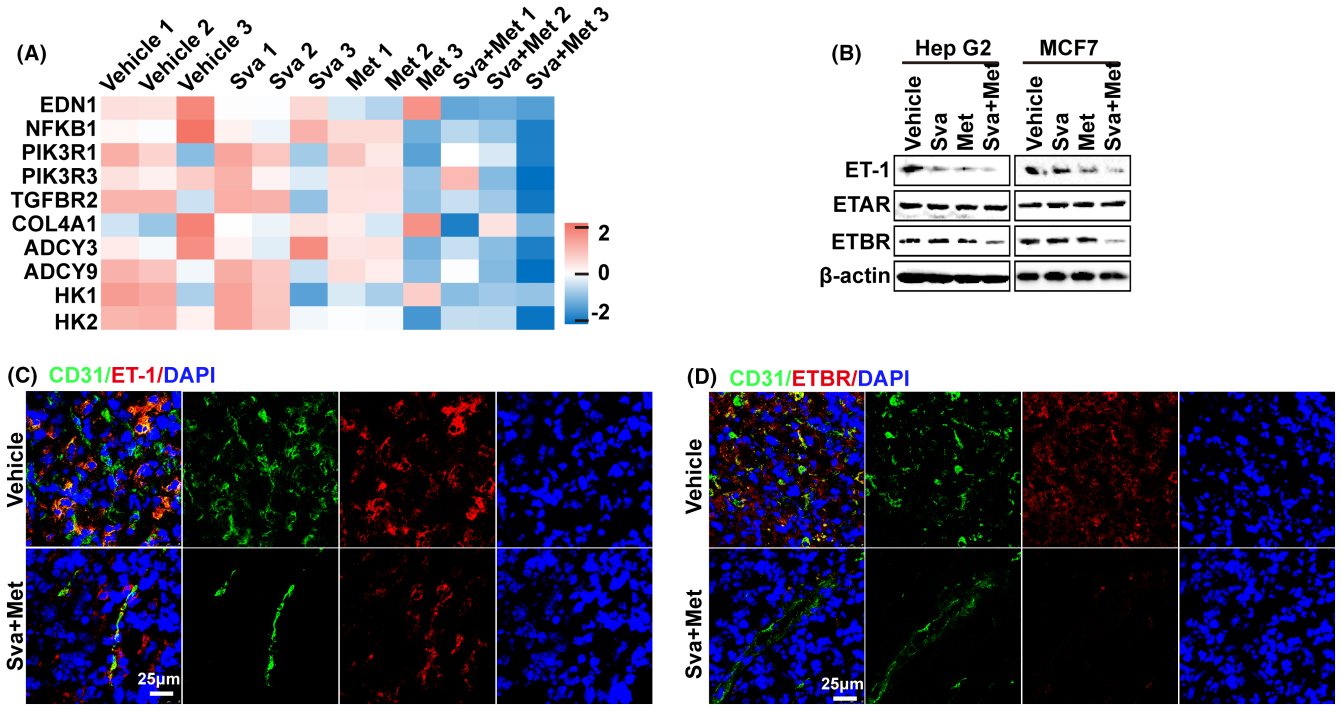

FIGURE 5 The effects of MET and SVA on hypoxia and ET-1. (A) Heat map of hypoxia-related genes in the indicated SVA and MET treatment groups. (B) Western blotting of ET-1, ETAR, and ETBR in HepG2 and MCF7 cells treated as indicated. Immunofluorescence of CD31 (green) and ETBR (red) of frozen sections of 4T1 tumors (C) and B16 tumors (D) from the indicated treatment groups. Bar = 25 μm. $^{**}P < 0.01$, $^{***}P < 0.001$.

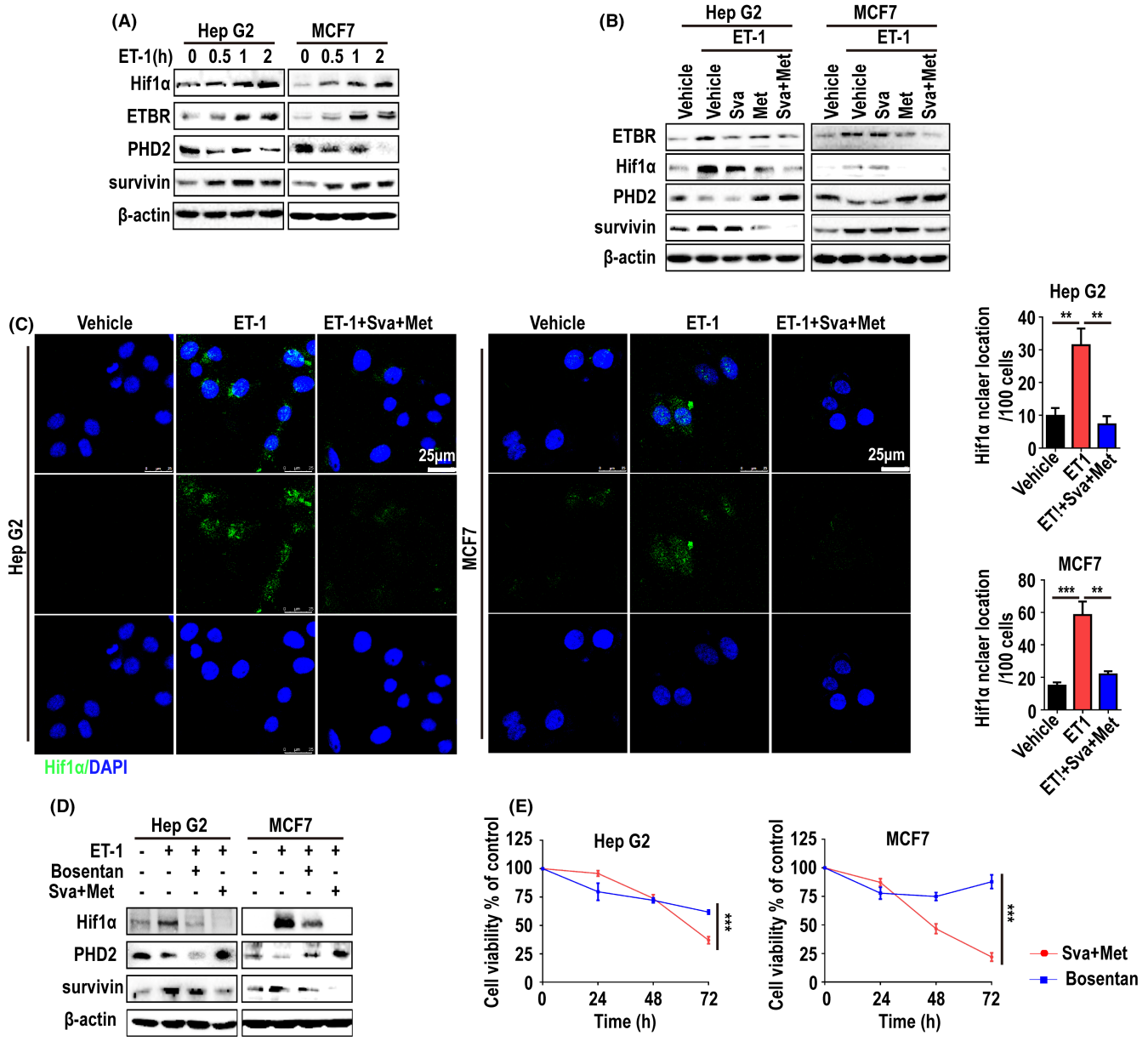

FIGURE 6 MET and SVA combination treatment inhibits the ET-1-ETBR-HIF1α signaling axis. (A) Western blot analysis of HIF1α, ETBR, PHD2, and survivin in HepG2 and MCF7 cells treated with 100 nM endothelin 1 for 0, 0.5, 1, or 2 h. (B) Western blot analysis of HIF1α, ETBR, PHD2, and survivin in HepG2 and MCF7 cells pre-treated with 100 nM (ET-1) for 1 h and then treated with SVA and/or MET for 24 h. (C) Immunofluorescence of HIF1α (green) in HepG2 cells with 100 nM (ET-1) pretreatment followed by SVA and/or MET treatment. Bar = 25 μm. (D) Western blot analysis of HIF1α, ETBR, PHD2, and survivin in HepG2 and MCF7 cells pretreated with 100 nM (ET-1) for 1 h and then treated with 100 nM bosentan or SVA and MET for 24 h. (D) Western blot analysis of HIF1α, ETBR, PHD2, and survivin in HepG2 and MCF7 cells pretreated with 100 nm (ET-1) for 1 h and then treated with 100 nm bosentan or SVA and MET for 24 h. (E) Cell viability curve of HepG2 and MCF7 cells after treatment with SVA and MET or bosentan for 24, 48, or 72 h.

downregulates hypoxia-induced ET-1 expression, consequently influencing the HIF1α and ET-1 feedback loop, is unknown, and we plan to examine this question in our next study.

The therapeutic blockade of ETBR is an attractive strategy for antitumor treatment, and several clinical studies have explored endothelin receptor antagonists as potential candidates for cancer therapy.[34] Bosentan is an ETBR antagonist that is used in the treatment of pulmonary arterial hypertension. A phase II trial exploring the use of bosentan in metastatic melanoma is ongoing.[41,57] Notably, our findings showed that the MET and SVA combination treatment showed similar effects on the regulation of ET-1-induced HIF1α downregulation and PHD2 upregulation as bosentan in both tumor cells and breast cancer PDOs. These findings support the possibility of the MET and SVA combination and its inhibition of the ET-1-HIF1α axis as a potential therapeutic strategy for antitumor treatment. However, our results were derived from only eight breast cancer PDOs and therefore more tumors and more tumor types are needed to further our findings.

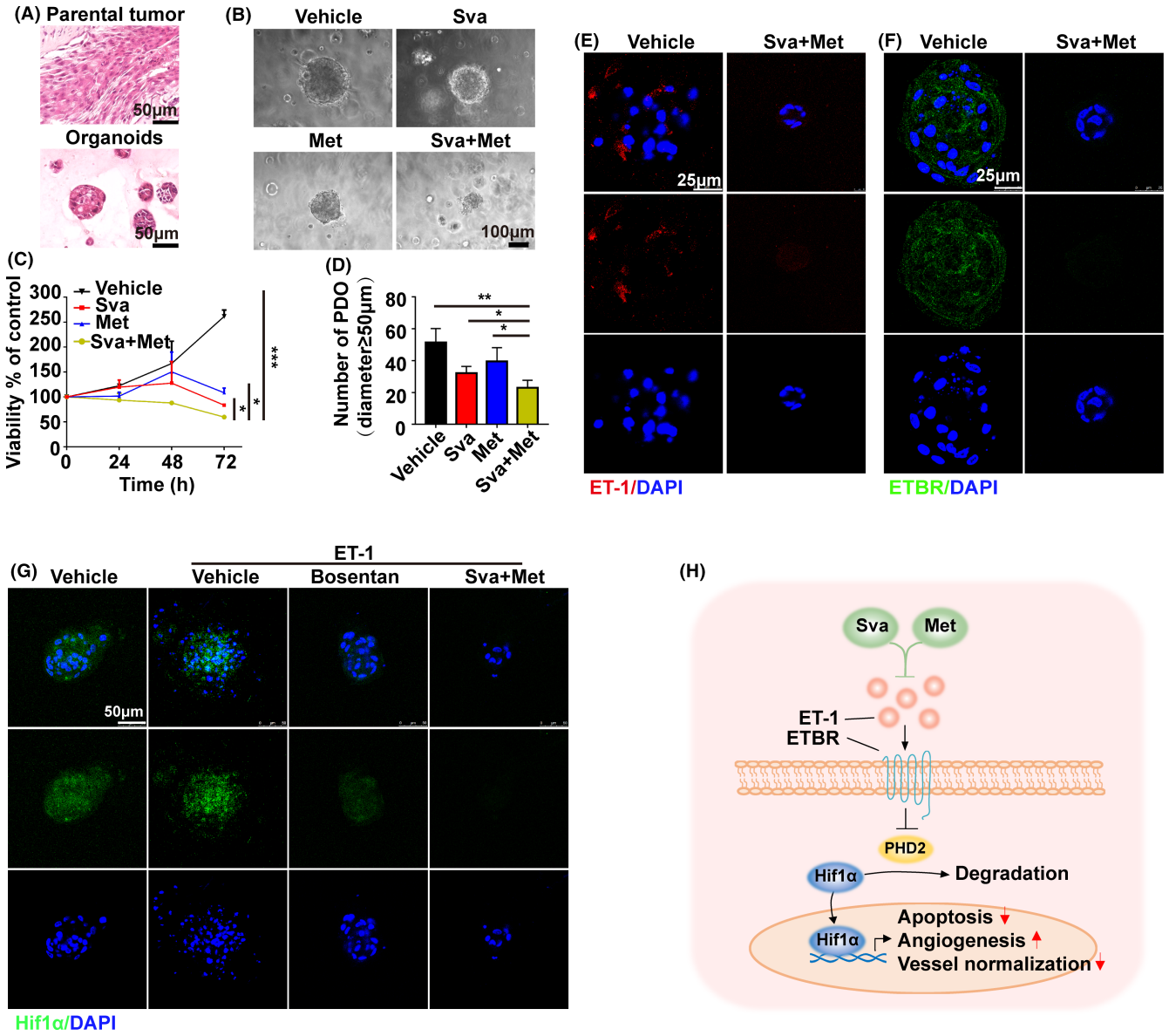

FIGURE 7 MET and SVA combination inhibits the growth of breast cancer patient-derived organoid (PDOs) and ETBR and HIF1α expression. (A) Hematoxylin and eosin staining of primary breast cancer tumor and PDO. Bar = 50 μm. (B) Images of PDOs treated with SVA and/or MET for 72 h. The viability (C) and volume (D) of breast cancer PDOs (diameter ≥ 50 μm) treated as indicated for 72 h. Immunofluorescence of ET-1 (E, red) and ETBR (F, green) in PDO treated with SVA and/or MET for 72 h. Bar = 25 μm. (G) Immunofluorescence of HIF1α (green) in PDOs pretreated with 100 nm (ET-1) for 1 h and then treated with 100 nm bosentan or SVA and MET. Bar = 50 μm. (H) Schematic model. The SVA and MET combination regulates the ET-1-ETBR-HIF1α signaling axis to induce apoptosis, inhibit angiogenesis, and promote vessel normalization.

Notably, our work identifies the MET and SVA combination as a more effective antitumor strategy compared with the ETBR antagonist bosentan. The development and approval of new drugs face many challenges in terms of effort, time, and expense, and drug development research is often accompanied by a high failure rate. Drug repurposing, in which drugs are applied for medical conditions other than their original indication, has emerged as a critical and valuable strategy for drug research and development.[58] MET and SVA are first-line clinical medications that are widely used for reducing hyperglycemia and hyperlipemia, respectively. Importantly, the safety and tolerability of both drugs have been tested and well established. Our findings therefore have great value in establishing MET and SVA as a potential and powerful anticancer strategy, reducing the time and cost of research and development.

The MET and SVA combination exerts its antitumor effects by alleviating hypoxia and decreasing angiogenesis. Importantly, improvement of the tumor hypoxic microenvironment and reduction of angiogenesis can increase the sensitivity of chemotherapy, radiotherapy, and tumor immunotherapy,[4,59–61] therefore we speculate that application of the combination treatment of MET and SVA together with chemotherapy, radiotherapy, or immunotherapy may have powerful therapeutic effects and improve patient prognosis.

AUTHOR CONTRIBUTIONS

Jie Liu, Peijun Liu, Juan Li, and Yu Ren conceived and designed the experiments. Jie Liu, Huxia Wang, Miao Zhang, Yazhao Li, Ruiqi Wang, He Chen, Xiaoqian Gao, and Shaoran Song performed the experiments and analyzed the data. Bo Wang and Yaochun Wang contributed reagents and materials. Jie Liu wrote the manuscript. All authors read and approved the final manuscript.

ACKNOWLEDGEMENT

This study was supported by the National Natural Science Foundation of China (No. 81703002 and 81872272), Key Research and Development Program of Shaanxi (No. 2020SF-038 and 2021SF-121) and Clinical Research Award of the First Affiliated Hospital of X'an Jiaotong University, China (No. XJTU1AF-CRF-2017-007).

CONFLICT OF INTEREST

The authors have no conflict of interest. All authors have read the journa's authorship agreement, and the manuscript has been reviewed by and approved by all named authors.

DATA AVAILABILITY STATEMENT

The data that support the findings of this study are available from the corresponding author upon reasonable request.

ETHICS STATEMENT

Our study was performed with the approval of the Ethics Committee of the First Affiliated Hospital of Xi'an Jiaotong University. Written informed consent was obtained from every patient.

ORCID

Yaochun Wang https://orcid.org/0000-0003-3498-3407
Peijun Liu https://orcid.org/0000-0002-0767-0774

REFERENCES

1. Conway EM, Collen D, Carmeliet P. Molecular mechanisms of blood vessel growth. *Cardiovasc Res*. 2001;49(3):507-521.
2. Folkman J. Angiogenesis: an organizing principle for drug discovery? *Nat Rev Drug Discov*. 2007;6(4):273-286.
3. Pugh CW, Ratcliffe PJ. Regulation of angiogenesis by hypoxia: role of the HIF system. *Nat Med*. 2003;9(6):677-684.
4. Keith B, Johnson RS, Simon MC. HIF1alpha and HIF2alpha: sibling rivalry in hypoxic tumour growth and progression. *Nat Rev Cancer*. 2011;12(1):9-22.
5. Petrova V, Annicchiarico-Petruzzelli M, Melino G, Amelio I. The hypoxic tumour microenvironment. *Oncogenesis*. 2018;7(1):10.
6. Viallard C, Larrivee B. Tumor angiogenesis and vascular normalization: alternative therapeutic targets. *Angiogenesis*. 2017;20(4):409-426.
7. Crawford Y, Ferrara N. VEGF inhibition: insights from preclinical and clinical studies. *Cell Tissue Res*. 2009;335(1):261-269.
8. Escudier B, Eisen T, Stadler WM, et al. Sorafenib in advanced clear-cell renal-cell carcinoma. *N Engl J Med*. 2007;356(2):125-134.
9. Lee J, Yesilkanal AE, Wynne JP, et al. Effective breast cancer combination therapy targeting BACH1 and mitochondrial metabolism. *Nature*. 2019;568(7751):254-258.
10. Cha JH, Yang WH, Xia W, et al. Metformin promotes antitumor immunity via endoplasmic-reticulum-associated degradation of PD-L1. *Mol Cell*. 2018;71(4):606-620 e607.
11. Liu J, Li J, Chen H, et al. Metformin suppresses proliferation and invasion of drug-resistant breast cancer cells by activation of the hippo pathway. *J Cell Mol Med*. 2020;24(10):5786-5796.
12. Wang JC, Li GY, Wang B, et al. Metformin inhibits metastatic breast cancer progression and improves chemosensitivity by inducing vessel normalization via PDGF-B downregulation. *J Exp Clin Cancer Res*. 2019;38(1):235.
13. Demierre MF, Higgins PD, Gruber SB, et al. Statins and cancer prevention. *Nat Rev Cancer*. 2005;5(12):930-942.
14. Li J, Liu J, Liang Z, et al. Simvastatin and atorvastatin inhibit DNA replication licensing factor MCM7 and effectively suppress RB-deficient tumors growth. *Cell Death Dis*. 2017;8(3):e2673.
15. Liang Z, Li W, Liu J, et al. Simvastatin suppresses the DNA replication licensing factor MCM7 and inhibits the growth of tamoxifen-resistant breast cancer cells. *Sci Rep*. 2017;7:41776.
16. Wang JC, Li XX, Sun X, et al. Activation of AMPK by simvastatin inhibited breast tumor angiogenesis via impeding HIF-1alpha-induced pro-angiogenic factor. *Cancer Sci*. 2018;109(5):1627-1637.
17. Juarez D, Fruman DA. Targeting the mevalonate pathway in cancer. *Trends Cancer*. 2021;7:525-540. doi:10.1016/j.trecan.2020.11.008
18. Sachs N, de Ligt J, Kopper O, et al. A living biobank of breast cancer organoids captures disease heterogeneity. *Cell*. 2018;172(1–2):373-386 e310.
19. Hanahan D, Weinberg RA. Hallmarks of cancer: the next generation. *Cell*. 2011;144(5):646-674.
20. Faubert B, Solmonson A, DeBerardinis RJ. Metabolic reprogramming and cancer progression. *Science*. 2020;368(6487):eaaw5473.
21. Partridge L, Fuentealba M, Kennedy BK. The quest to slow ageing through drug discovery. *Nat Rev Drug Discov*. 2020;19(8):513-532.
22. Sirtori CR. The pharmacology of statins. *Pharmacol Res*. 2014;88:3-11.
23. Adak T, Samadi A, Unal AZ, et al. A reappraisal on metformin. *Regul Toxicol Pharmacol*. 2018;92:324-332.
24. Llovet JM, Zucman-Rossi J, Pikarsky E, et al. Hepatocellular carcinoma. *Nat Rev Dis Primers*. 2016;2:16018.
25. Shweiki D, Itin A, Soffer D, Keshet E. Vascular endothelial growth factor induced by hypoxia may mediate hypoxia-initiated angiogenesis. *Nature*. 1992;359(6398):843-845.
26. Folkman J. Role of angiogenesis in tumor growth and metastasis. *Semin Oncol*. 2002;29(6 Suppl 16):15-18.
27. Kerbel RS. Tumor angiogenesis. *N Engl J Med*. 2008;358(19):2039-2049.
28. Ebos JM, Kerbel RS. Antiangiogenic therapy: impact on invasion, disease progression, and metastasis. *Nat Rev Clin Oncol*. 2011;8(4):210-221.
29. Goel S, Duda DG, Xu L, et al. Normalization of the vasculature for treatment of cancer and other diseases. *Physiol Rev*. 2011;91(3):1071-1121.
30. Soriano AF, Helfrich B, Chan DC, Heasley LE, Bunn PA, Chou TC. Synergistic effects of new chemopreventive agents and conventional cytotoxic agents against human lung cancer cell lines. *Cancer Res*. 1999;59(24):6178-6184.
31. Arami S, Mahdavi M, Rashidi MR, et al. Apoptosis induction activity and molecular docking studies of survivin siRNA carried by Fe3O4-PEG-LAC-chitosan-PEI nanoparticles in MCF-7 human breast cancer cells. *J Pharm Biomed Anal*. 2017;142:145-154.
32. Ambrosini G, Adida C, Altieri DC. A novel anti-apoptosis gene, survivin, expressed in cancer and lymphoma. *Nat Med*. 1997;3(8):917-921.
33. Wheatley SP, Altieri DC. Survivin at a glance. *J Cell Sci*. 2019;132(7):jcs223826.
34. Rosano L, Spinella F, Bagnato A. Endothelin 1 in cancer: biological implications and therapeutic opportunities. *Nat Rev Cancer*. 2013;13(9):637-651.

35. Spinella F, Rosano L, Del Duca M, et al. Endothelin-1 inhibits prolyl hydroxylase domain 2 to activate hypoxia-inducible factor-1alpha in melanoma cells. *pLoS One*. 2010;5(6):e11241.
36. Caprara V, Scappa S, Garrafa E, et al. Endothelin-1 regulates hypoxia-inducible factor-1alpha and -2alpha stability through prolyl hydroxylase domain 2 inhibition in human lymphatic endothelial cells. *Life Sci*. 2014;118(2):185-190.
37. Peng XH, Karna P, Cao Z, Jiang BH, Zhou M, Yang L. Cross-talk between epidermal growth factor receptor and hypoxia-inducible factor-1alpha signal pathways increases resistance to apoptosis by up-regulating survivin gene expression. *J Biol Chem*. 2006;281(36):25903-25914.
38. Chen YQ, Zhao CL, Li W. Effect of hypoxia-inducible factor-1alpha on transcription of survivin in non-small cell lung cancer. *J Exp Clin Cancer Res*. 2009;28(1):29.
39. Motte S, McEntee K, Naeije R. Endothelin receptor antagonists. *Pharmacol Ther*. 2006;110(3):386-414.
40. Kefford RF, Clingan PR, Brady B, et al. A randomized, double-blind, placebo-controlled study of high-dose bosentan in patients with stage IV metastatic melanoma receiving first-line dacarbazine chemotherapy. *Mol Cancer*. 2010;9:69.
41. Kefford R, Beith JM, Van Hazel GA, et al. A phase II study of bosentan, a dual endothelin receptor antagonist, as monotherapy in patients with stage IV metastatic melanoma. *Invest New Drugs*. 2007;25(3):247-252.
42. van de Wetering M, Francies HE, Francis JM, et al. Prospective derivation of a living organoid biobank of colorectal cancer patients. *Cell*. 2015;161(4):933-945.
43. Meng J, Zhu Y. Efficacy of simvastatin plus metformin for polycystic ovary syndrome: a meta-analysis of randomized controlled trials. *Eur J Obstet Gynecol Reprod Biol*. 2021;257:19-24.
44. Babcook MA, Sramkoski RM, Fujioka H, et al. Combination simvastatin and metformin induces G1-phase cell cycle arrest and Ripk1- and Ripk3-dependent necrosis in C4-2B osseous metastatic castration-resistant prostate cancer cells. *Cell Death Dis*. 2014;5:e1536.
45. Kim JS, Turbov J, Rosales R, Thaete LG, Rodriguez GC. Combination simvastatin and metformin synergistically inhibits endometrial cancer cell growth. *Gynecol Oncol*. 2019;154(2):432-440.
46. Seo Y, Kim J, Park SJ, et al. Metformin suppresses cancer stem cells through AMPK activation and inhibition of protein prenylation of the mevalonate pathway in colorectal cancer. *Cancers (Basel)*. 2020;12(9):2554.
47. Antwi SO, Li Z, Mody K, Roberts LR, Patel T. Independent and joint use of statins and metformin by elderly patients with diabetes and overall survival following HCC diagnosis. *J Clin Gastroenterol*. 2020;54(5):468-476.
48. Babcook MA, Shukla S, Fu P, et al. Synergistic simvastatin and metformin combination chemotherapy for osseous metastatic castration-resistant prostate cancer. *Mol Cancer Ther*. 2014;13(10):2288-2302.
49. Liu SH, Yu J, Creeden JF, et al. Repurposing metformin, simvastatin and digoxin as a combination for targeted therapy for pancreatic ductal adenocarcinoma. *Cancer Lett*. 2020;491:97-107.
50. Jimenez-Vacas JM, Herrero-Aguayo V, Montero-Hidalgo AJ, et al. Clinical, cellular, and molecular evidence of the additive antitumor effects of biguanides and statins in prostate cancer. *J Clin Endocrinol Metab*. 2021;106(2):e696-e710.
51. Del Campo JA, Garcia-Valdecasas M, Gil-Gomez A, et al. Simvastatin and metformin inhibit cell growth in hepatitis C virus infected cells via mTOR increasing PTEN and autophagy. *pLoS One*. 2018;13(1):e0191805.
52. Wang JC, Sun X, Ma Q, et al. Metformi's antitumour and anti-angiogenic activities are mediated by skewing macrophage polarization. *J Cell Mol Med*. 2018;22:3825-3836. doi:10.1111/jcmm.13655
53. Nelson J, Bagnato A, Battistini B, Nisen P. The endothelin axis: emerging role in cancer. *Nat Rev Cancer*. 2003;3(2):110-116.
54. Spinella F, Rosano L, Di Castro V, et al. Endothelin-1 and endothelin-3 promote invasive behavior via hypoxia-inducible factor-1alpha in human melanoma cells. *Cancer Res*. 2007;67(4):1725-1734.
55. Platero-Luengo A, Gonzalez-Granero S, Duran R, et al. An O2-sensitive glomus cell-stem cell synapse induces carotid body growth in chronic hypoxia. *Cell*. 2014;156(1–2):291-303.
56. Hisada T, Ayaori M, Ohrui N, et al. Statin inhibits hypoxia-induced endothelin-1 via accelerated degradation of HIF-1alpha in vascular smooth muscle cells. *Cardiovasc Res*. 2012;95(2):251-259.
57. Russo A, Bronte G, Rizzo S, et al. Anti-endothelin drugs in solid tumors. *Expert Opin Emerg Drugs*. 2010;15(1):27-40.
58. Strittmatter SM. Overcoming drug development bottlenecks with repurposing: old drugs learn new tricks. *Nat Med*. 2014;20(6):590-591.
59. Chouaib S, Noman MZ, Kosmatopoulos K, Curran MA. Hypoxic stress: obstacles and opportunities for innovative immunotherapy of cancer. *Oncogene*. 2017;36(4):439-445.
60. Munn LL, Jain RK. Vascular regulation of antitumor immunity. *Science*. 2019;365(6453):544-545.
61. Lytle NK, Barber AG, Reya T. Stem cell fate in cancer growth, progression and therapy resistance. *Nat Rev Cancer*. 2018;18(11):669-680.

SUPPORTING INFORMATION

Additional supporting information can be found online in the Supporting Information section at the end of this article.

How to cite this article: Liu J, Wang H, Zhang M, et al. Metformin and simvastatin synergistically suppress endothelin 1-induced hypoxia and angiogenesis in multiple cancer types. *Cancer Sci*. 2023;114:640-653. doi: 10.1111/cas.15602